Journal of Fluorescence (2025) 35:4143–4155
https://doi.org/10.1007/s10895-024-03819-1

RESEARCH

Spectral Characteristics of Water-Soluble Rhodamine Derivatives for Laser-Induced Fluorescence

Abhishek Ratanpara[1] · Myeongsub Kim[1] · Yeo Jun Kim[2] · Carlos H. Hidrovo[3]

Received: 19 April 2024 / Accepted: 24 June 2024 / Published online: 2 July 2024

Abstract

We present a comprehensive fluorescence characterization of seven water-soluble rhodamine derivatives for applications in laser-induced fluorescence (LIF) techniques. Absorption and emission spectra for these dyes are presented over the visible spectrum of wavelengths (400 to 700 nm). Their fluorescence properties were also investigated as a function of temperature for LIF thermometry applications. Rhodamine 110 depicted the least fluorescence emission sensitivity to temperature at -0.11%/°C, while rhodamine B depicted the most with a -1.55%/°C. We found that the absorption spectra of these molecules are independent of temperature, supporting the notion that the temperature sensitivity of their emission only comes from changes in quantum yield with temperature. Conversely, these rhodamine fluorophores showed no change in emission intensities with pH variations and are, therefore, not suitable tracers for pH measurements. Similarly, fluorescent lifetime, which is also a property sensitive to local environmental changes in temperature, pH, and ion concentration, measurements were conducted for these fluorophores. It was found that rhodamine B and kiton red 620 have shorter fluorescence timescales compared to those of the other five rhodamine dyes, making them least suitable for applications where temporal changes in emission are monitored. Lastly, we conducted experiments to assess the physicochemical absorption characteristics of these dyes' molecules into polydimethylsiloxane (PDMS), the most common material for microfluidic devices. Rhodamine B showed the highest diffusion into PDMS substrates as compared to the other derivative dyes.

Keywords Rhodamine · Water-soluble · Laser induced fluorescence · Temperature sensitivity · pH · PDMS diffusion

Introduction

Many physical and engineering applications, such as the assessment of heat transfer characteristics in fluid flows and visualization of species mixing, often involve the use of fluorescent dyes since these tracers can probe the physical parameters associated with these phenomena [1–6]. Laser-induced fluorescence (LIF), a versatile tool for the visualization and quantification of changes in temperature [1, 7], pH [8, 9], and local concentrations [10–12], is well equipped for these purposes. Fluorescence in LIF is an inelastic radiative process involving the absorption and subsequent emission of a photon following quantum energy state interactions. By measuring fluorescence emissions from dye molecules affected by environmental conditions, LIF can be used to construct a local spatiotemporal map of these quantities.

The selection of the most suitable fluorophores is an important step in the optimization and characterization of any LIF system [13, 14]. However, this selection process is usually costly and time-consuming since multiple tests are involved that require considerable amounts of materials and equipment in order to accurately determine the properties of the chosen fluorophores. The comprehensive study presented here, which examines the absorption and emission characteristics of a family of dyes according to environmental conditions, can be used to assess the accuracy

✉ Myeongsub Kim
kimm@fau.edu

Carlos H. Hidrovo
hidrovo@neu.edu

[1] Ocean and Mechanical Engineering, Florida Atlantic University, 777 Glades Road, Boca Raton, FL 33431, USA

[2] Multiscale Thermal Fluids Laboratory, Mechanical Engineering Department, The University of Texas at Austin, 204 E. Dean Keeton, Austin, TX 78712, USA

[3] Multiscale Thermal Fluids Laboratory, Mechanical and Industrial Engineering Department, Northeastern University, 360 Huntington Ave, Boston, MA 02114, USA

and suitability of the different fluorophores for specific LIF applications.

Rhodamine derivatives are the most popular fluorophores suitable for LIF since they have several excellent photochemical properties compared to other fluorescent molecules [15–20]. Some desirable properties of rhodamine derivatives are that (1) they absorb a broad band of wavelengths covering the 400 –650 nm range (i.e., they allow flexibility in terms of excitation sources) [21], (2) their quantum yields are relatively high compared to other fluorophores (~30% higher), such as fluorescein [21–24], and (3) they are highly resistant to photobleaching (a phenomenon by which a dye loses its ability to fluoresce under extended photoexcitation) [25–27]. Generally, they are photochemically stable in dry powder form in dark environments, but they have also shown great promise as indicators of physical properties when they are dissolved in hydrocarbon-based solvents such as ethanol and methanol [28]. Hence, their absorption and emission spectra in hydrocarbon solutions are extensively available in the literature [28–34]. While these hydrocarbon-based solvents provide high solubility of the rhodamine dyes, many chemical and engineering applications require different solvents, such as water, glycerol, deuterium oxide, and dimethyl sulfoxide.

Water can undoubtedly be considered the cleanest solvent available, greatly contributing to "green chemistry" [35]. In addition, water is essential in organic chemistry for synthesis and reactions [36]. The advantages of using water as a solvent include fast reaction rates, non-toxicity, and low cost. It is also nonflammable and environmentally friendly and can prevent the dissolution of organic gases, which are major considerations in air-sensitive catalysis [35]. For aqueous-based LIF applications, water-soluble fluorophores that can probe changes in system properties are required. Water-soluble rhodamine derivatives are a great choice for this purpose due to the aforementioned advantages. While some studies have used one or two specific water-soluble rhodamine dyes for temperature or concentration measurements [12, 17, 37], there is no study that extensively compares the absorption and emission spectra of the many available water-soluble rhodamine derivatives and systematically quantifies their pH and temperature-dependent characteristics.

In this paper, we present spectral characteristics of seven water-soluble rhodamine derivatives whose emissions cover most of the visible wavelengths $\lambda = 420$ –650 nm. Their absorption and fluorescence spectra were obtained at room temperature when dissolved in deionized (DI) water. The temperature sensitivities of these rhodamine derivatives were also obtained in the 26–55 °C range. Our most important conclusion was that the absorption spectra of rhodamine derivatives are independent of temperature. This implies that the temperature sensitivity of the fluorescence emission presumably comes from changes in their quantum yields with temperature rather than their absorption spectra. Similarly, their fluorescence emissions were characterized as a function of pH. For a demonstration of pH-dependent emissions of rhodamine derivatives, a CO_2 dissolution-driven pH change was induced in DI water for fluorescein and rhodamine B solutions in a PMMA-based microchannel. In addition, their fluorescent lifetimes, a key parameter in LIF applications for cancer research [38], human skin disease [39], and stem cell research [40], were characterized. Finally, using fluorescence microscopy, the absorption and diffusion of these rhodamine derivatives in PDMS, a representative material used in aqueous LIF applications, were also measured.

This study provides spectral characteristics of water-soluble rhodamine dyes, including their absorption and emission spectra as a function of temperature and pH, fluorescence lifetimes, and diffusion behaviors into PDMS. While some of this information can be found in various papers on LIF systems, this report gathers all the data on different rhodamine derivatives into one place, making it a valuable and unique resource.

Experimental Methods

Instruments

The absorption spectra at room temperature were measured by a CARY 5000UV-VIS NIR spectrophotometer (Varian, USA) with an excitation slit of 1 nm. All measurements carried out with this instrument were calibrated by the absorption spectrum of a base solvent. Emission spectra at room temperature were recorded on a FluoroLog®-3 spectrofluorometer (HORIBA Scientific, USA) with a 450 W xenon CW lamp as the illumination source. A clear, four-sided, 1 cm cuvette was used with a 420 nm excitation source alongside a 1 nm emission slit for spectra collection. The fluorescence was measured at 90° to the incident excitation beam from 450 nm to 700 nm. The fluorescence intensities were calibrated against the fluorescence of the base solvent (water in this study) and the detector response. Temperature-dependent absorption and emission spectra were measured by a SpectraMax microplate reader (Molecular Devices, USA). Using fluorophore solutions at a 10 µM concentration, eight fluorophores, including Fl and seven rhodamine derivatives, were transferred to a 96-well plate. The microplate reader provides automatic calibration for background noise and temperature-controlled measurements. Measurements were made for each temperature after the microplate reader was auto-calibrated against a built-in thermocouple.

Reagents and Materials

DI water was prepared by removing contaminants from tap water with a filtration system. All rhodamine derivatives were purchased from Exciton (Exciton Inc., USA) and used as received. Both sodium phosphate monobasic and dibasic were purchased from Sigma. Citric monohydrate and sodium hydroxide were obtained from Fisher Scientific.

Preparation of pH Solution

To produce a pH 8.5 fluorophore solution, 0.1 M phosphate sodium salt was dissolved in DI water. An appropriate amount of fluorophore solution at 5 µmol/L from the 1 mmol/L stock was then added to the pH buffer. It should be noted that the concentration of fluorescence solution must be chosen to be low to avoid the effect of reabsorption of surrounding dyes' fluorescence. To produce a pH 6.5 solution, sodium hydroxide was used to titrate the pH of the DI water. To produce a pH 4.5 solution, 0.1 M citric acid and sodium hydroxide were used to titrate the pH values similarly as described above.

Measurement of Fluorescence Lifetime

For fluorescent lifetime measurements, changes in time-dependent photon counts were recorded by the Fluoro-Log®-3 spectrofluorometer under ambient conditions. A four-sided clear cuvette containing the fluorophore solution was placed into a holder, and a diode laser at 421 nm excited the sample with a bandwidth of 1 nm. A photomultiplier measured the number of photons from the sample at 20 kHz with an emission bandwidth of 1 nm. By exciting the sample with the laser at a repetition rate of 10 MHz, time-resolved measurements of fluorescence lifetime were made. Specifically, time-correlated single photon counting was recorded based on the detection of the arrival times of individual photons to the photomultiplier immediately after the 300ps laser pulse excitation commences. This excitation-emission process was repeated many times by building up a histogram of the number of counts versus time.

Diffusion of dye Molecules into PDMS

Polydimethylsiloxane (PDMS) is a permeable material to gas and organic molecules. It is well known that RhB, an organic fluorescent dye, significantly diffuses into cured PDMS. In this study, diffusion and absorption of seven rhodamine derivatives, including RhB, into PDMS was visualized and quantified by fluorescence microscopy. After curing PDMS microchannels, they were placed on a microscope stage so that the field of view was the same for each chip. A 10 µM aqueous dye solution was then injected by a syringe pump at 10 µL/min. A reference image at $t = 0$ s was taken immediately after the solution was injected, and a second image was taken 60 min later. Fluorescence emissions from each dye solution throughout the microchannel section and adjacent wall sections were recorded by a 10x objective lens onto a CCD camera.

CO_2 Dissolution-induced pH Change

DI water with the 10 µM concentration of fluorescein (FL 116) and rhodamine B (RH 115), respectively, were used to test their pH sensitivity. The pH of aqueous solutions was changed by continuous CO_2 dissolution as the CO_2-water reaction produces two hydrogen ions from the subsequent dissociation of dissolved CO_2 (*aq*). To test the pH sensitivity of different dyes, a polymethylmethacrylate (PMMA) microchannel (100 µm (W)×100 µm (H) ×30 mm (L)), possessing excellent optical access to imaging of fluorescence, was prepared (Fig. 1). Each test solution was injected into the PMMA microchannel with a syringe pump with a 90 µL volume. Once the channel was filled halfway through with the test solution, the outlet port was closed while the inlet was immediately connected to a CO_2 gas line (the gas valve had not been turned on at this point). It is important that the time step to switch the water line to the gas line

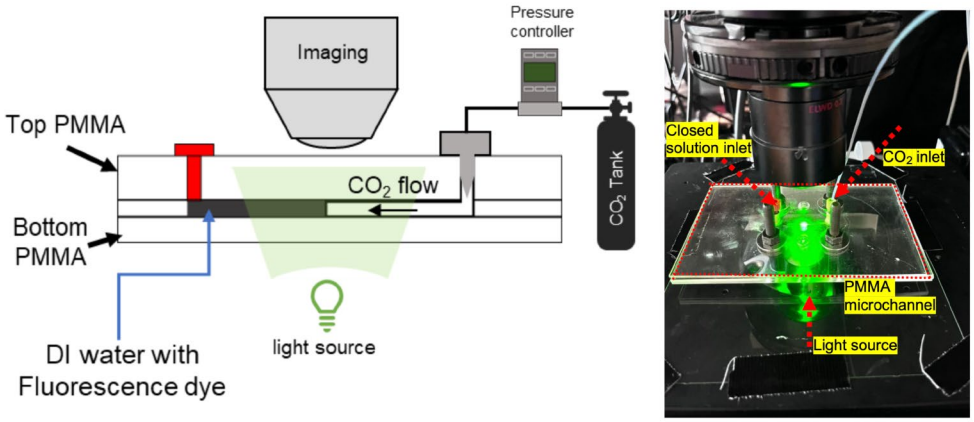

Fig. 1 An illustrative experimental diagram for the CO_2 dissolution-induced pH changes of fluorescein and rhodamine B solutions in a PMMA microchannel (left side). A photograph of the actual experimental setup (right)

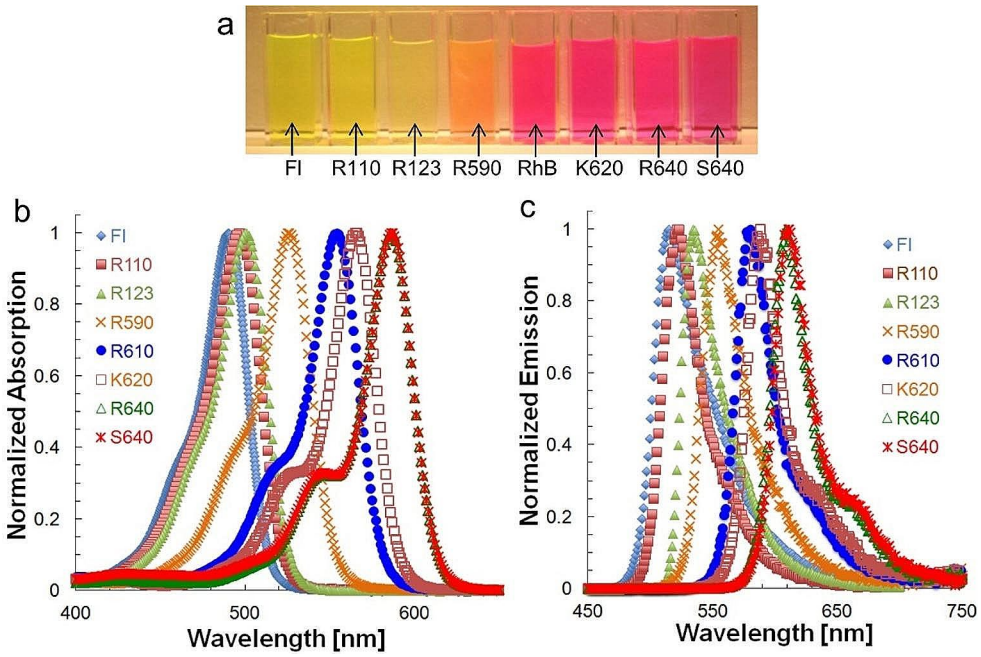

Fig. 2 (**a**) A photograph, (**b**) absorption spectra, and (**c**) emission spectra for fluorescein and seven rhodamine derivatives

Table 1 Absorption and emission maximum for Fl and seven rhodamine dyes

Dye	Fl	R110	R123	R590	RhB	K620	R640	S640
Wavelength at absorption maximum (nm)	490	496	500	526	554	565	586	586
Wavelength at emission maximum (nm)	515	521	534	554	580	588	609	610

must be as short as possible because CO_2 dissolution started before the imaging began. The solution-filled microchannel was exposed to 0.5 psig CO_2 gas over time when the gas pressure was maintained constant during the test. The time-dependent emission intensities were recorded by a camera for image processing.

Results and Discussion

Absorption and Emission Spectra

Figure 2a shows an image depicting Fl (yellow-green) and seven rhodamine derivatives: (rhodamine 110 (R110), rhodamine 123 (R123), rhodamine 590 (R590), rhodamine 610 (R610 or RhB), kiton red 620 (K620), rhodamine 640 (R640), and sulforhodamine 640 (S640)) under ambient light conditions at 21 °C. Fl, a popular fluorophore for use in LIF, was chosen as a baseline for comparison purposes. The color of the rhodamine derivatives ranges from yellow-green (R123) to dark pink (S640), indicating that their emissions range from ~500 nm to ~600 nm. Although R123, R110, and Fl are discernable in the figure, RhB, K620, R640, and S640 are difficult to distinguish by color due to the similarity of their emission spectra.

Figure 2b and c show absorption and emission spectra for Fl and seven rhodamine derivatives at a 10 μM concentration, while their maximum absorption and emission values are tabulated in Table 1. For the rhodamine derivatives, the seven dyes combined cover a wavelength range from 420 nm to 650 nm. It is noteworthy that four of these fluorophores, R610, K620, R640, and S640, have a second absorption peak at a shorter wavelength, making their absorption range broader than other similar dyes. This second absorption peak characteristic also results in a second peak of fluorescence at longer wavelengths (Fig. 2c). These broadening effects are beneficial, especially when these fluorophores are employed in LIF techniques because (1) there is more flexibility in the selection of the excitation sources (e.g., Ar + laser at 488, 514 nm, Nd: YAG laser at 532 nm), and (2) various combinations of fluorophores are possible in dual-tracer applications by minimizing crosstalk between two wavelength bands [1, 7].

Temperature and pH Dependence

LIF provides a practical, non-invasive approach to measuring liquid temperatures that has been extensively used in different applications [1, 7, 37]. The temperature-dependent characteristics on the quantum yield of some dye molecules allow for thermometry by monitoring the fluorescence intensity changes with temperature. To accurately measure temperatures using LIF, it is essential to carefully choose the appropriate temperature-sensitive tracers. Figure 3

shows the temperature-dependent fluorescence spectra for Fl and the seven rhodamine derivatives picked in this study. All spectra were obtained in a temperature-controlled spectrometer (SpectraMax, USA) at 27, 35, 45 and 55 °C. It is well known that Fl is a good temperature tracer with a strong temperature-sensitive emission [1], as seen in Fig. 3 (a). The temperature sensitivity of the rhodamine dyes varies depending on the specific fluorophore. The emission of Rhodamine 110 shows no temperature dependence, suggesting that this dye serves as a good reference dye when no temperature sensitivity is desired. On the other hand, all the other derivatives show temperature-dependent emissions, with a uniform decrease in intensity across the emission

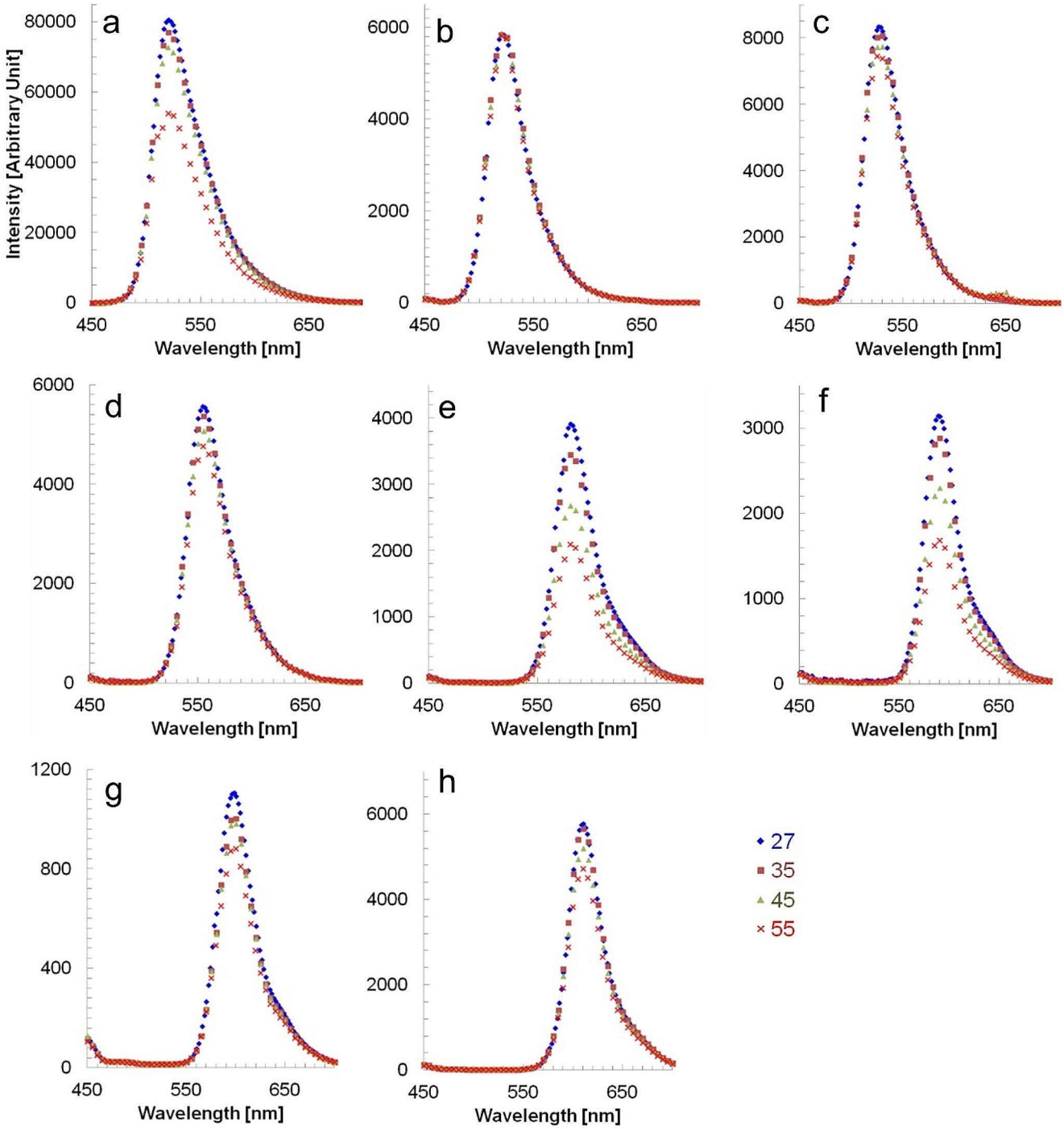

Fig. 3 Emission spectra for fluorescein and rhodamine derivatives at different temperatures: (**a**) Fl, (**b**) R110, (**c**) R123, (**d**) R590, (**e**) R610, (**f**) K620, (**g**) R640, and (**h**) S640

Table 2 Changes in emissions of Fl and rhodamine derivatives with temperatures and their average temperature sensitivity in the range of 27–55 °C

	Fl	R110	R123	R590	R610	K620	R640	S640
% change of emission maximum*	33.1	0.4	10.6	14.5	46.5	46.4	20.3	18.3
% change in total emission (based on area)*	31.5	3.3	9.2	14.3	45.0	44.6	18.8	16.1
Temperature Sensitivity (%/°C)**	-1.08	-0.11	-0.31	-0.49	-1.55	-1.53	-0.64	-0.55

*Temperature changes from 27 to 55 °C

**When curve-fitted to a linear

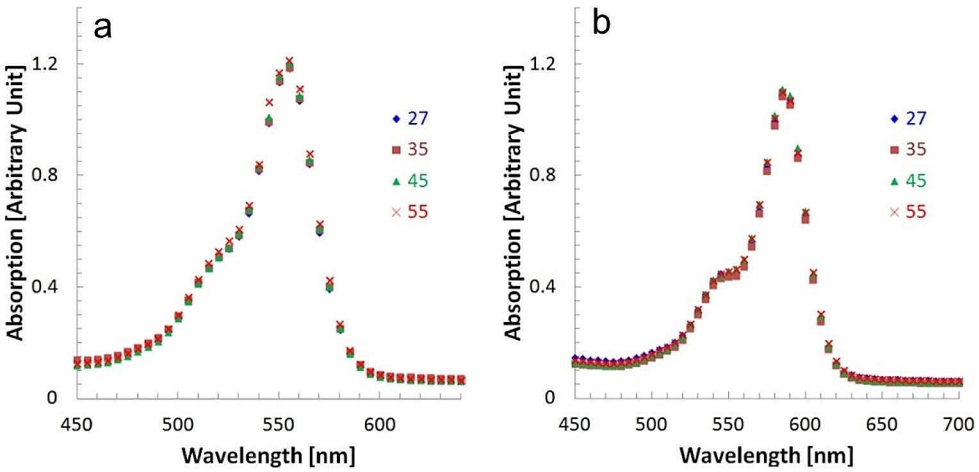

Fig. 4 Absorption spectra of R610 and S640 at different temperatures

spectrum but without distortion or shift on its wavelength profile.

Table 2 shows quantitative results of changes in both the emission maximum and the total amount of emission as temperatures change from 26 °C to 55 °C. There are very slight differences in the exact percentage change between the peak fluorescence intensity and the sum of the total emission intensities as a function of temperature, mostly due to experimental error, but the overall characteristics of change are essentially the same. Fl shows about 31% change of emission, resulting in a temperature sensitivity of -1.08%/°C. Among the rhodamine derivatives, the dyes that show the largest changes in their emissions are R610 and K620, showing a temperature sensitivity of -1.55 and − 1.53%/°C, respectively. These sensitivities are in agreement with the literature [1, 7]. It should be noted that the correlation of temperature with fluorescence intensity for various dyes is not always linear but often polynomial, as referenced in the literature [41]. If a dual fluorescence LIF approach is to be used, a tracer pair combination of a temperature-sensitive dye and a temperature-insensitive dye is typically required. By taking the ratio of two emissions, the source of errors due to fluctuation of excitation intensity can be minimized. As long as both dyes are excitable by the same illumination source, it is apparent that the combination of R610-R110 shows the highest temperature sensitivity and, therefore, provides the most accurate temperature measuring system.

Temperature-dependent fluorescence occurs because either the quantum yield or the fluorophore's absorption spectrum is sensitive to temperature changes. Fl is a well-known fluorophore with different temperature sensitivities when excited at different wavelengths due to its temperature-sensitive absorption characteristics [1]. For example, Fl has a temperature sensitivity of -0.16%/°C when excited at 488 nm, while it has 2.43%/°C at 514 nm excitation. To investigate the effect of temperature on the fluorescence of the rhodamine derivatives, their absorption spectra were measured at temperatures of 27, 35, 45, and 55 °C. Figure 4 shows representative absorption spectra for R610 and S640 dyes. It is apparent from Fig. 4 that the absorption spectra of all derivatives are insensitive to temperature. These results support the notion that the temperature sensitivity of their emissions is unaffected by the excitation wavelength. Rather, the emissions change with temperature, apparently due to variations in quantum yield with temperature. It should be noted that the variation in quantum yield is partially due to the variation of the solution's viscosity with temperature [42]. The explanation of how the quantum yield of fluorophore changes with temperature is mentioned in many kinds of literature. The quantum yield of a fluorophore changes with temperature due to several interconnected factors. As temperature increases, molecular vibrations enhance non-radiative decay processes, causing energy loss as heat instead of fluorescence [43]. Additionally, the solvent's viscosity decreases, facilitating rotational

and vibrational motions that quench fluorescence [43]. Higher temperatures also lead to more frequent collisions between fluorophore and solvent molecules, promoting non-radiative relaxation [44]. In varied molecular environments, fluorophores may undergo structural changes with temperature, altering their electronic environment and affecting fluorescence properties [45] Furthermore, temperature variations can influence energy transfer processes, such as Förster Resonance Energy Transfer (FRET), by modifying the distance between donor and acceptor molecules, thereby affecting the fluorescence quantum yield [43]. Understanding these mechanisms requires specific experimental data and detailed analysis, including fluorescence lifetimes and temperature-dependent spectroscopy, to fully consider the fluorophore's physical and chemical environment. While these aspects are important, this manuscript focuses solely on the spectral characteristics of the fluorophores.

Another important aspect to consider when using organic fluorescent molecules as tracers for measurements of physical properties is their sensitivity to solution pH. Changes in pH cause variations in emission intensities due to the pH-dependent absorptivity of the dye molecules. Figure 5 shows the emission spectra for the representative rhodamine dyes R123 and S640 that exhibit emission characteristics independent of solution pH over the 4.5, 6.5, and 8.5 values. Although rhodamine dyes are a good choice as tracers for temperature measurements in environments with variable pH conditions, other organic fluorophores, such as Fl, are better choices for pH measurements. We want to point out that this conclusion is solely from the observations of emission spectra with temperature.

As one of the representative demonstrations for pH measurements with these dyes, we measured pH changes in DI water with fluorescein and rhodamine B upon continuous CO_2 injection into test solutions. Because of cascading hydrogen ion production from CO_2-water reactions, the carbonated solution by CO_2 becomes acidic, lowering the solution pH. Figure 6(a) and (b) show changes in emission intensities of both fluorescein and rhodamine B dyes at 6 different time steps along the microchannel when the solution was pressurized by a CO_2 gas. In the case of fluorescein dye, the emission changed from the meniscus (not shown in the figure) of the CO_2-water interface. Since a CO_2 gas continuously dissolves into the test solution (from the right-hand side of the figure), the solution pH becomes acidic. Figure 6(a) shows an intensity decrease of fluorescein's emission over time due to its pH sensitivity. On the other hand, emission intensities of rhodamine B remained constant over time upon CO_2 injection, as expected, because of the pH-insensitivity of its emission intensity.

Fluorescence Lifetime

Fluorescence lifetime (τ), defined as the average time that a molecule resides in the excited state before returning to its ground state, is an intrinsic property of the fluorophore. Due to the high sensitivity of the fluorescence lifetime to environmental conditions, measurements of the fluorophore's lifetime can be used to evaluate changes in pH [46–49], temperature [50–52], and ion concentration [53, 54]. For example, Sanders et al. [46]. used the ratio of fluorescence lifetime measurements in two different time windows to map pH values over Chinese hamster ovary cells with a carboxy SNAFL-1 whose fluorescence lifetime is pH-dependent. Similarly, Nakabayashi et al. [49] used fluorescence lifetime imaging microscopy (FLIM) to image the intracellular pH of HeLa cells by using the pH-dependent ionic equilibrium of the chromophore from enhanced green fluorescent proteins. In order to measure intercellular temperature distributions in a living COS7 cell, Okabe et al. [51] employed the temperature-dependent fluorescent lifetime of a fluorescent polymeric thermometer that diffuses throughout the entire cell, combined with a time-correlated single photon counting system-based FLIM. In addition, Tremier et al. [55] utilized FLIM to determine fluorescence resonance energy transfer (FRET) in living cells as a powerful method for visualizing protein-protein interactions and biochemical reactions. They studied the impact of photobleaching on

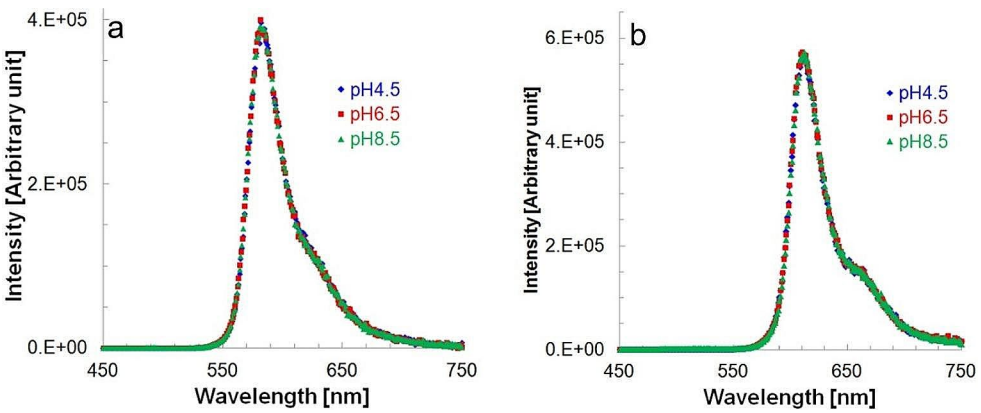

Fig. 5 Emission spectra of R123 and S640 at different solution pH

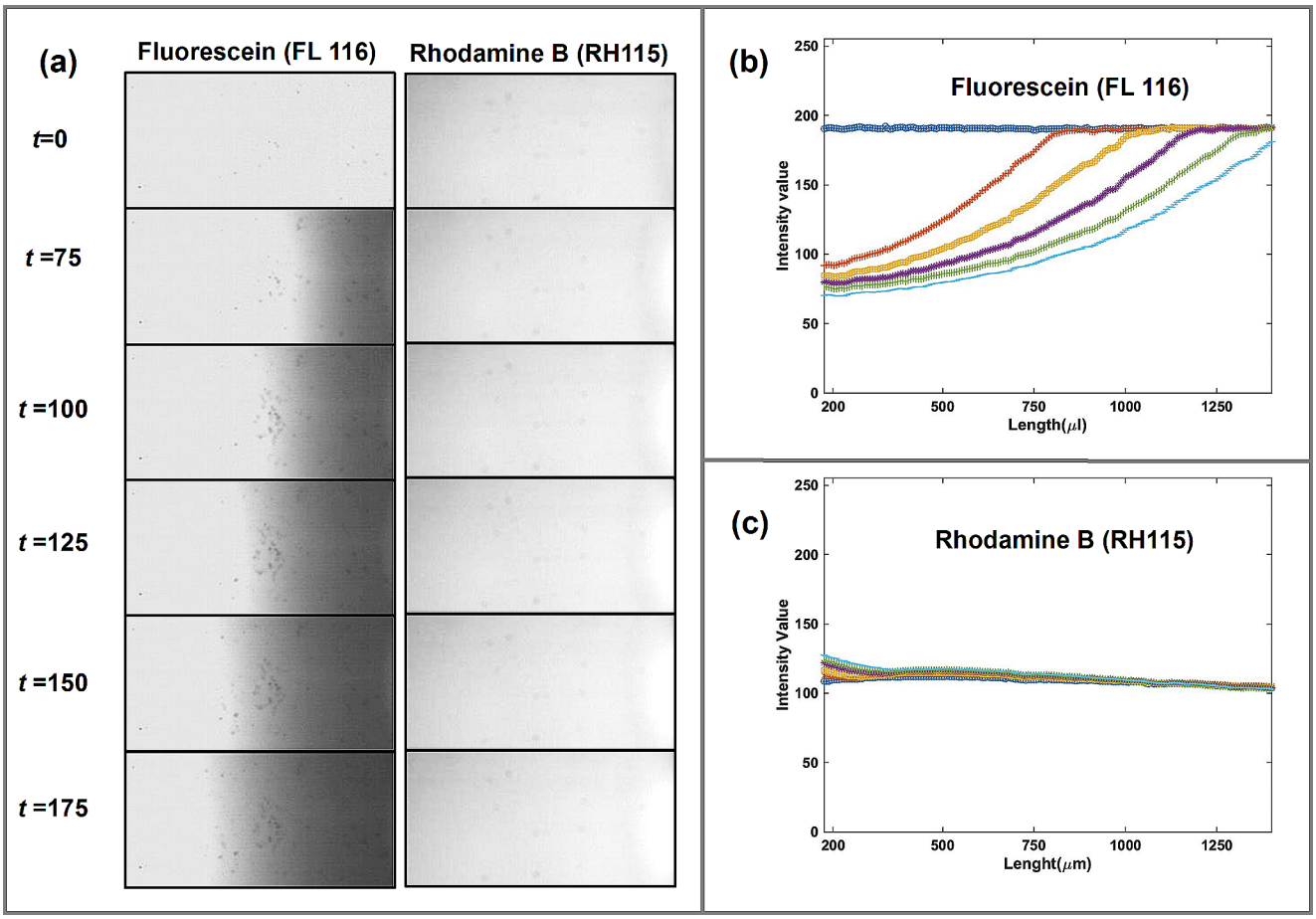

Fig. 6 pH-sensitive emissions of rhodamine B and fluorescein dyes (**a**) Greyscale images at 6 different time steps during CO_2 dissolution in fluorescein and rhodamine B dyes in DI water in a PMMA microchannel (**b**, **c**) Time-dependent emission profiles along the channel for (**b**) fluorescein (FL 116) and (**c**) rhodamine B (RH 115)

the measured fluorescent lifetime from fluorescent proteins such as CFP, YFP, and GFP in FRET applications. Lastly, Bopp et al. [56] used fluorescence lifetime measurement to estimate the photobleaching time of one bacteriochlorophyll molecule by using a confocal fluorescence microscope with picosecond time resolution.

Fluorescence emission occurs when the excited fluorophore molecules return to their ground state, releasing energy in the form of visible light. This process and the corresponding fluorescence intensity follow an exponential decay over time that can be expressed as:

$I(t) = I_0 \exp(-t/\tau)$,

where I_0 is the maximum intensity of the fluorescent emission at the population inversion point. The fluorescence lifetime is defined as the time taken for this peak fluorescence intensity to decay to $1/e$ (37%) of its value. Although fluorescence derives from a stochastic excitation-relaxation process, its intensity initially increases as the number of molecules that populate the excited state increases until reaching its maximum intensity, I_o, at the onset of the population inversion point before gradually decaying.

In the current study, we measured the fluorescence lifetime of the seven rhodamine derivatives under the same environmental conditions, specifically room temperature (23 °C), atmospheric pressure, and pH 6.5. Figure 7 shows the fluorescence lifetime measurements for Fl and the seven rhodamine dyes in DI water. It is apparent that there are two distinct groups of fluorescence lifetimes for the rhodamine dyes: one for RhB and K620 and another one for the rest of the rhodamine derivatives (Table 3). These results indicate that the emissions of RhB and K620 have shorter decay times (less than 1.74 ns) than the other rhodamine dyes (decay times of 4.53 ns and more). Due to the large range in fluorescence lifetimes (1.71 ns to 5.08 ns), in terms of absolute lifetime values, these rhodamine derivatives seem comparable to the fluorophores used in the aforementioned applications above. For example, the lifetime of carboxy SNAFL-1 is 1.1 ns, while those of GFP and YFP are 3.5

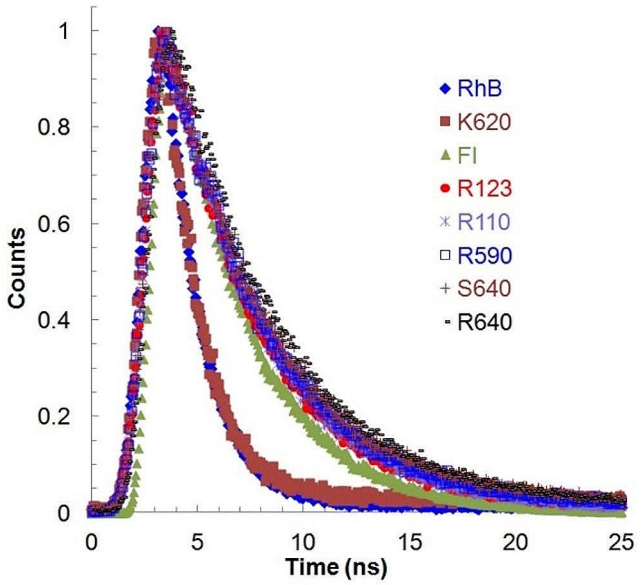

Fig. 7 Fluorescence lifetime measurements for Fl and seven water-soluble rhodamine dyes

and 4.5 ns, respectively. However, to ensure that these rhodamine dyes are competitive against these other tracers for the purposes of measuring environmental pH and temperature changes, further work on the dependence of their fluorescent lifetimes as a function of these variables is needed.

Diffusion into PDMS

PDMS-based chips are well suited to LIF techniques due to their transparency and ease of fabrication [57, 58]. However, they have been shown to have issues with absorption and diffusion of small molecules into their surfaces and bulk [59, 60]. However, to date, no study has compared the quantitative degree of permeability of rhodamine derivatives into PDMS microchannels. To test their permeability into the PDMS material, each of the seven rhodamine derivatives was mixed in solution with DI water at a concentration of 10 µM and injected into a 100 µm-square PDMS microchannel. Two fluorescence images of the microchannel were taken at 0 and 60 min after the solution was injected at a flow rate of 10 µL/min. Figure 8 shows greyscale images of the fluorescence emission when RhB was injected into the chip at 0 min (Fig. 8a), depicting no initial absorption or diffusion of the dye solution into the PDMS and after 60 min (Fig. 8b). By continuing to expose the microchannel to the RhB solution, a large amount of RhB molecules start to permeate into the PDMS walls and subsequently penetrate the PDMS bulk, producing a smoother fluorescence profile that gradually decays from the wall to the interior of the sample. After 60 min of injection, it is apparent that significant diffusion of RhB molecules into the PDMS material has occurred, as shown in Fig. 8b. To quantify and compare the degree of diffusion between the seven rhodamine molecules, the intensity profiles at $t = 60$ min were analyzed against the profile at $t = 0$ min as shown in Fig. 8c. As can be seen in the figure, the intensity profile of RhB is more pronounced towards the PDMS bulk material as compared to the others, suggesting that the diffusion of these molecules is more significant. Quantitatively, RhB penetrates the PDMS material up to 30% of the microchannel width, while the others penetrate the PDMS bulk by only 5% of its width.

Fluorescent Dyes in Temperature and pH Measurements Measurement

In Table 4, we have summarized some published studies highlighting various types of fluorescent dyes sensitive to pH and temperature. These studies showcase the diverse applications and behaviors of fluorescent dyes across different pH and temperature ranges. By encompassing these data, we provide an overview of how these dyes respond to environmental changes, which is crucial for selecting the appropriate dye for specific experimental conditions.

Table 3 Fluorescence lifetime for Fl and seven rhodamine dyes

Dye	Fl	RhB	K620	R123	R110	R590	S640	R640
Fluorescence Lifetime (ns)	3.74	1.71	1.74	4.53	4.66	4.80	4.92	5.08

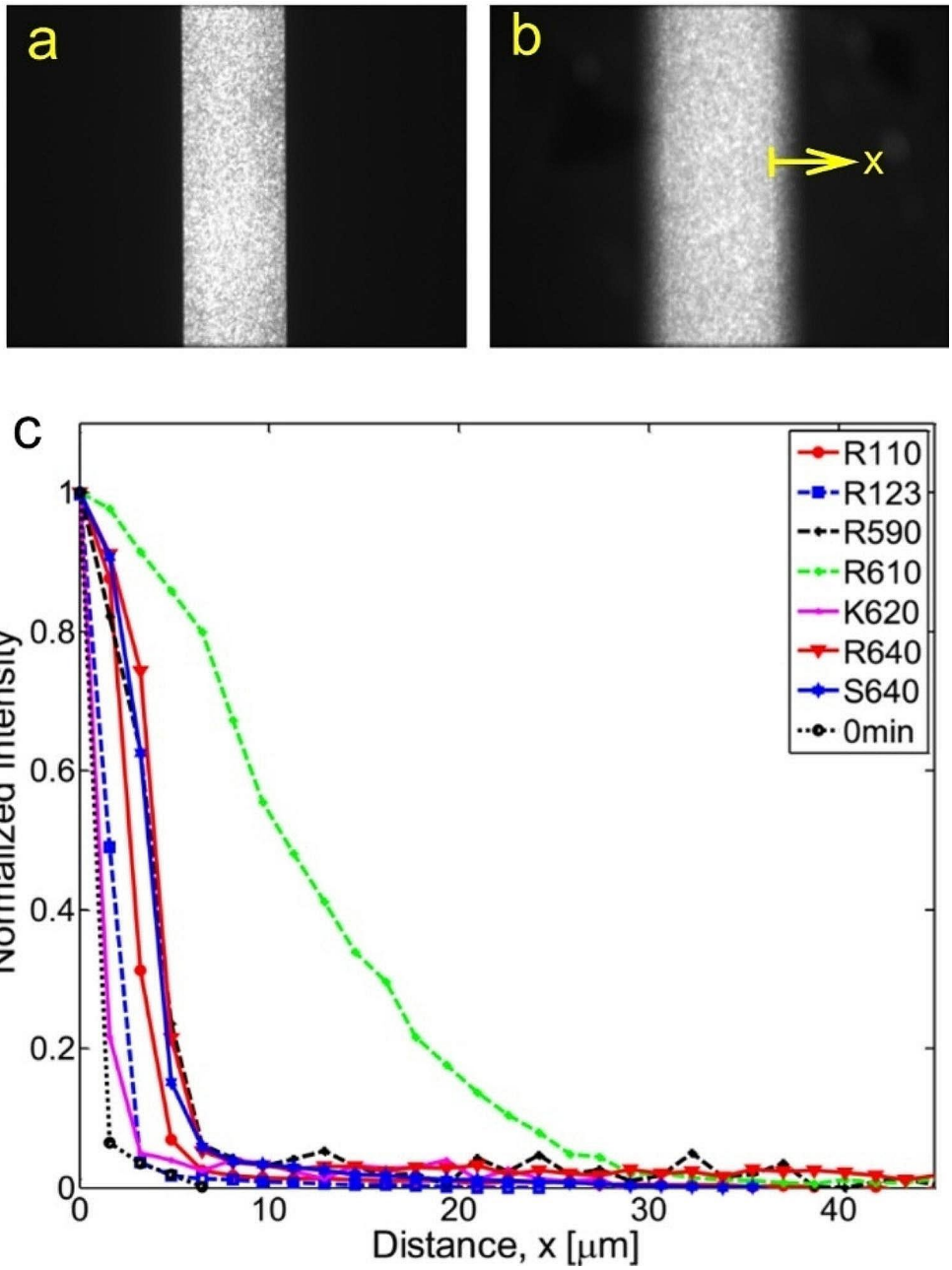

Fig. 8 Greyscale channel images at 0 min (**a**) and 60 min (**b**) after RhB was injected. (**c**) Intensity profiles at 60 min of injection along the line in (**b**) from the PDMS-water interface

Table 4 Recent studies on measurements of pH and temperature with various fluorophores

Study	Dye	Applications	Temperature and pH Measurement Range	Reference
1	Fluorescein and Rhodamine B	Droplet Thermometry	20–60 °C	[61]
2	5(6)-Carboxyfluorescein	Thermochromic Liquid Crystals	15–75 °C	[62]
3	2',7'-Dichlorofluorescein	Microfluidics Temperature Sensing	10–80 °C	[63]
4	Fluorescein Isothiocyanate (FITC)	Biological Temperature Probes	15–75 °C	[64]
5	Fluorescein-O-Methacrylate	Polymer-Based Temperature Sensors	20–90 °C	[65]
6	Fluorescein Diacetate	Various Temperature Measurements	5–80 °C	[66]
7	5(6)-Carboxyfluorescein	pH and Temperature Sensing	2–8	[67]
8	Fluorescein and Rhodamine B	Bioimaging	4–8	[68]
9	6-Carboxyfluorescein	Thermochromic Liquid Crystals	3–9	[69]

Conclusion

LIF is a versatile tool that can non-intrusively measure several physical parameters such as temperature, pH, and concentration using organic fluorophores. Water is often used as a solvent in this technique due to its low cost and biocompatibility. This study measured the absorption and fluorescence characteristics of seven water-soluble rhodamine dyes for their use in different LIF applications. These molecules' absorption and fluorescence spectra were measured in the 26–55 °C range for temperature measurement application. We found that rhodamine B has the strongest temperature dependence with −1.55%/°C. We also found that the temperature sensitivity of the emissions of all rhodamine derivatives comes from changes in quantum yield with temperatures rather than absorptivity. Conversely, the rhodamine fluorophores tested showed no change in emission intensities with pH variation, suggesting that these rhodamine derivatives are not appropriate options for pH measurements. We demonstrated pH-dependent emissions of fluorescein and rhodamine B using CO_2-induced pH change of the solution. Fluorescent lifetime measurements of the dyes showed that rhodamine B and kiton red 620 had a shorter timescale compared to the other five dyes, suggesting that these latter ones might provide a better dynamic range in FLIM measurements. Furthermore, the lifetimes from the rhodamine family span the timescales of other common tracers, making them a viable alternative for aqueous applications. It must be noted that since we tested the temperature- and pH-sensitive emission spectra for various fluorophores, the impact of the time-dependent laser intensity must be considered when the users use these dyes for LIF applications. Finally, it was found that rhodamine B shows the strongest propensity to diffusion into PDMS, suggesting that this dye should be avoided in applications employing this material, while no significant penetration of the other dyes to PDMS was observed after one hour, making them more appropriate for these purposes.

Author Contributions A.R.: methodology, testing, data acquisition, data curation, writing-original draft preparation. M.M.: supervision, conceptualization, methodology, testing, data acquisition, data curation, writing-original draft preparation, reviewing, and editing. Y.K.: methodology, testing, data acquisition, data curation. C.H.: supervision, conceptualization, methodology, data curation, writing - reviewing, and editing.

Funding This work was supported by an NSF CAREER Award grant CBET- 1151091.

Data Availability No datasets were generated or analysed during the current study.

Declarations

Ethical Approval Not applicable as the study does not include any use of animals and humans.

Consent to Publish All authors mentioned in the manuscript have consented to submission and publication.

Competing Interests The authors declare no competing interests.

References

1. Coppeta J, Rogers C (1998) Dual emission laser induced fluorescence for direct planar scalar behavior measurements Exp. Fluids 25:1–15
2. Kim M, Yoda M (2012) Extending fluorescence thermometry to measuring wall surface temperatures using evanescent-wave illumination ASME J. Heat Transf 134:011601
3. Kim M, Sell A, Sinton S (2013) Aquifer-on-a-Chip: understanding pore-scale salt precipitation dynamics during CO 2 sequestration. Lab Chip 13:2508–2518
4. Caroll B, Hidrovo C 2012 Droplet collision mixing diagnostics using single fluorophore LIF exp. Fluids 53 1301–1316
5. Pfeiffer SA, Sagl S (2015) Microfluidic platorms employing integrated fluorescence or luminescent chemical sensors: a refiew of methods, scope and applicatios methods Appl. Fluoresc 3:034003
6. Hofmann J, Meier RJ, Mahnke A, Schatz V, Brackmann F, Trollmann R, Bogdan C, Liebsch, Wang XD, Wolfbeis OS, Jantsch J 2015 Ratiometric luminescence 2D in vivo imaging and monitoring of mouse skin osygenation methods Appl. Fluoresc. 4 045002

7. Kim M, Yoda M (2010) Dual-tracer fluorescence thermometry measurements in a heated channel Exp. Fluids 49:257–266
8. Shinohara K, Sugii Y, Okamoto K, Madarame H, Hibara A, Tokeshi M, Kitamori T (2004) High-speed micro-PIV measurements of transient flow in microfluidic devices Meas. Sci Technol 15:1965–1970
9. Munkholm C, Walt D, Milanovich F, Klainer S (1986) Polymer modification of fiber optic chemical sensors as a method of enhancing fluorescence signal for pH. Meas Anal Chem 58:1427–1430
10. Lozano A, Yip B, Hanson RK (1992) Acetone: a tracer for concentration measurements in gaseous flows by planar laser-induced fluorescence exp. Fluids 13:369–376
11. Sun S, Ungerbock, Mayr T (2015) Imaging of oxygen in microreactors and microfluidic systems methods Appl. Fluoresc 3:034002
12. Arcoumanis C, McGuirk JJ, Palma J M L M 1990 on the use of fluorescent dyes for concentration measurements in water flows Exp. Fluids 10 177–180
13. Hidrovo CH, Hart DP (2001) Emission reabsorption laser induced fluorescence (ERLIF) film thickness measurement Meas. Sci Technol 12:467–477
14. Sakakibara J, Adrian RJ (1999) Whole field measurement of temperature in water using two-color laser induced fluorescence exp. Fluids 26:7–15
15. Wilkcrson CW Jr, Goodwin PM, Ambrose WP, Martin JC, Keller RA (1993) Detection and lifetime measurement of single molecules in flowing sample streams by laser-induced fluorescence Appl. Phys. Lett. 62 2030
16. Hishida K, Sakakibara J (2000) Combined Planar laser-induced fluorescence–particle image velocimetry technique for velocity and temperature fields Exp. Fluids 29:S129–S140
17. Kisley L, Chang WS, Copper D, Mansur AP, Landes CF (2013) Extending single molecule fluorescence observation time by amplitude-modulated excitation methods Appl. Fluoresc 1:037001
18. Gu P, Birch DJS, Chen Y (2014) Dye-doped polystyrene-coated gold nanorods: towards wavelength tunable SPASER methods Appl. Fluoresc 2:024004
19. Muhlfriedel K, Baumann KH (2000) Concentration measurements during mass transfer across liquid-phase boundaries using planar laser induced fluorescence (PLIF) exp. Fluids 28:279–281
20. Dovichi NJ, Martin JC, Jett JH, Keller R a 1983 Attogram detection limit for aqueous dye samples by laser-induced fluorescence. Science 219 845–847
21. Zhang XF, Zhang Y, Liu L (2014) Fluorescence lifetimes and quantum yields of ten rhodamine derivatives: structural effect on emission mechanism in different solvents. J Lumin 145:448–453
22. Beija M, Afonso CAM, Martinho JMG (2009) Synthesis and applications of rhodamine derivatives as fluorescent probes Chem. Soc Rev 38:2410–2433
23. Crosby GA, Demas JN (1971) Measurement of photoluminescence quantum yields. Rev J Phys Chem 75:991–1024
24. Kubin RF, Fletcher AN (1982) Fluorescence quantum yields of some rhodamine dyes J. Lumin 27:455–462
25. Kolmakov K, Belov VN, Bierwagen J, Ringemann C, Muller V, Eggeling C, Hell SW (2010) Red-emitting rhodamine dyes for Fluorescence Microscopy and Nanoscopy Chem. Eur J 16:158–166
26. Mohanty J, Nau WM (2005) Ultrastable Rhodamine with Cucurbituril Angew. Chem Int Ed 117:3816–3820
27. Eggeling C, Widengren J, Rigler R, Seidel CAM (1998) Photobleaching of fluorescent dyes under conditions used for single-molecule detection: evidence of two-step photolysis anal. Chem 70:2651–2659
28. Leytus SP, Melhado LL, Mangel WF (1983) Rhodamine-based compounds as fluorogenic substrates for serine proteinases Biochem. J 209:299–307
29. Sauer M, Han KT, Muller R, Nord S, Schulz A, Seeger S, Wolfrum J, Arden-Jacob J, Deltau G, Marx NJ Zander C and Drexhage K H 1995 New fluorescent dyes in the red region for biodiagnostics. J Fluoresc 5 247–261
30. Deshpande AV, Namdas EB (1997) Lasing action of rhodamine B in polyacrylic acid films. Appl Phys B 64:419–422
31. Baruah M, Qin W, Flors C, Hofkens J, Vallee RAL, Heljonne D, Auweraer MVD Borggraeve W M D and Boens N 2006 Solvent and pH dependent fluorescent properties of a dimethylaminostyryl borondipyrromethene dye in solution. J Phys Chem A 110 5998–6009
32. Wei Zhou X, Fang Q, Qiao W, Jiang Y, Zhang Z, Xu (2021) Quantitative assessment of rhodamine spectra. Chin Chem Lett Volume 32(2):943–946
33. Radiul SM, Chowdhury J, Hazarika S (2023) Fluorescent H-aggregates of pure rhodamine B (RhB) in glycerol, ethylene glycol, methanol and butanol under ambient condition. J Mol Struct Volume 1275:0022–2860
34. Radiul SM, Chowdhury J, Goswami A, Hazarika S (2022) Fluorescence spectroscopy based characterisation method for aggregation behaviour of rhodamine B (RhB) in water, ethanol, and propanol, laser physics, 32, issue 7
35. Dallinger D, Kappe CO (2007) Microwave-assisted synthesis in water as solvent Chem. Rev 107:2563–2591
36. Li CJ, Chen L (2006) Org Chem Water Chem Soc Rev 35:68–82
37. Ross D, Gaitan M, Locascio LE (2001) Temperature measurement in microfluidic systems using a temperature-dependent fluorescent dye Anal. Chem 73:4117–4123
38. Wang HW, Chen CT, Guo HW, Yu JS, Wei YH, Gukassyan C, Kao FJ (2008) Differentiation of apoptosis from necrosis by dynamic changes of reduced nicotinamide adenine dinucleotide fluorescence lifetime in live cells. J Biomed Opt 13:054011
39. Ehlers A, Riemann I, Stark M, Konig K 2007 Multiphoton fluorescence lifetime imaging of human hair Microsc. Res Techniq 70 154–161
40. Uchugonova A, Konig K 2008 two-photon autofluorescence and second-harmonic imaging of adult stem cells J. Biomed Opt 13 054068
41. Sharafy S, Muszkat KA (1971) Viscosity dependence of fluorescence quantum yield. J Am Chem Soc 93:17
42. Sharafy S, Muszkat KA Viscosity dependence of fluorescence quantum yield. J Am Chem Soc, 93, 17, 1971
43. Valeur B, Berberan-Santos MN (2012) Molecular fluorescence: principles and applications. Wiley
44. Haugland RP (2002) Handbook of fluorescent probes and Research Chemicals. Molecular Probes
45. Lakowicz JR (2006) Principles of fluorescence spectroscopy. Springer Science & Business Media
46. Sanders R, Draaijer A, Gerritsen HC, Houpt PM, Levine YK (1995) Quantitative pH imaging in cells using confocal fluorescence lifetime imaging microscopy Anal. Biochem 227:302–308
47. Hanson KM, Behne MJ, Barry NP, Mauro TM, Gratton E, Clegg RM (2002) Two-photon fluorescence lifetime imaging of the skin stratum corneum pH gradient Biopysic. J 83:1682–1690
48. Lin H, Herman P, Lakowicz JR (2003) Fluorescence lifetime-resolved pH imaging of living cells Cytom. Part A 52A:77–89
49. Nakabayashi T, Wang H, Kinjo M, Ohta N (2008) Application of fluorescence lifetime imaging of enhanced green fluorescent protein to intracellular pH measurements Photochem. Photobiol Sci 7:668–670
50. Kemnitz K, Nakashima N, Yoshihara K, Matsunami H (1989) Temperature dependence of fluorescence decays of isolated

rhodamine B molecules adsorbed on semiconductor single crystals. J Phys Chem 93:6704–6710
51. Okabe K, Inada N, Gota C, Harada Y, Funatsu T, Uchiyama S (2011) Intracellular temperature mapping with a fluorescent polymeric thermometer and fluorescence lifetime imaging microscopy Nature Comm. 3:1–9
52. Graham EM, Iwai K, Uchiyama S, Silva APD, Magennis SW, Jones AC Lab chip 2010 quantitative mapping of aqueous microfluidic temperature with sub-degree resolution using fluorescence lifetime imaging microscopy. Lab Chip 10 1267–1273
53. Lewkowicz A, Bojarski P, Synak A, Grobelna B, Akopova I, Gryczynski I, Kulak L 2012 concentration-dependent fluorescence properties of rhodamine 6G in titanium dioxide and silicon dioxide nanolayers. J Phys Chem C 116 12304–12311
54. Serra-Gomez R, Tardajos G, Gonzalez-Benito J, Gonzalez-Gaitano G (2012) Rhodamine solid complexes as fluorescence probes to monitor the dispersion of cyclodextrins in polymeric nanocomposites. Dyes Pigm 94:427–436
55. Tramier M, Zahid M, Mevel JC, Masse MJ, Coppey-Moisan M (2006) Sensitivity of CFP/YFP and GFP/mCherry pairs to donor photobleaching on FRET determination by fluorescence lifetime imaging microscopy in living cells Microsc. Res Techniq 69:933–939
56. Bopp MA, Jia Y, Li L, Cogdell RJ, Hochstrasser RM (1997) Fluorescence and photobleaching dynamics of single light-harvesting complexes Proc. Natl. Acad. Sci. USA 94 10630
57. Bliss CL, McMullin JN, Backhouse CJ (2008) Integrated wavelength-selective optical waveguides for microfluidic-based laser-induced fluorescence detection. Lab Chip 8:143–151
58. Tung YC, Zhang M, Lin CT, Kurabayashi K, Skerlos SJ (2004) PDMS-based opto-fluidic micro flow cytometer with two-color, multi-angle fluorescence detection capability using PIN photodiodes Sen. Actuat 98:356–367
59. Borysiak MD, Bielawski KS, Sniadecki NJ, Jenkel CF Vogt B D and Posner J D 2013 simple replica micromolding of biocompatible styrenic elastomers. Lab Chip 13 2773–2784
60. Samy R, Galwdel T, Ren CL (2008) Method for microfluidic whole-chip temperature measurement using thin-film poly (dimethylsiloxane)/Rhodamine B anal. Chem 80:369
61. Lakowicz JR, Masters BR (2008) Principles of fluorescence spectroscopy. J Biomed Opt 13(2):029901. https://www.sciencedirect.com/science/article/pii/S0894177717304272
62. Gryczynski I, Lakowicz JR, Malicka J (2009) Fluorescence sensing. Chem Rev 109(1):83–108. https://pubs.acs.org/doi/full/https://doi.org/10.1021/cr900249z
63. Harms T, Kessler S (2017) Two-color temperature and velocity field measurement in microfluidics using luminescence lifetime imaging. Experiments in Fluids, 58(8), 106. https://link.springer.com/article/10.1007/s00348-017-2475-y
64. Narayanaswamy R, Wolfbeis OS (2012) Optical sensors: industrial, environmental, and diagnostic applications. Sens Actuators B 168(1):122–132. https://www.sciencedirect.com/science/article/pii/S0263224112004605
65. Tsuji A, Ikeda T, Sugiyama M (2004) Temperature-sensitive fluorescence characteristics of fluoresceinamine-labeled copolymer gels in aqueous solution. Journal of Oceanography, 60(4), 693–699. https://link.springer.com/article/10.1007/s10872-004-5771-0
66. Wang X, Zuo YY (2023) Fluorescence detection of temperature changes in biological systems using a novel fluorescein derivative. J Photochem Photobiol A 424:113567. https://www.sciencedirect.com/science/article/pii/S1290072923005471
67. Koide Y, Urano Y, Hanaoka K, Terai T, Nagano T (2000) Development of an Si-rhodamine-based far-red to near-infrared fluorescence probe selective for hypoxic cells. Chem Commun 200015:1683–1684. https://pubs.rsc.org/en/content/articlehtml/2000/cc/b007108k
68. Haugland RP (2002) Handbook of fluorescent probes and research chemicals. Biotechniques 32(5):1192–1197. https://www.tandfonline.com/doi/full/10.2144/000112001
69. Breslow R (2004) Determining the geometries of transition states by use of antihydrophobic additives in water acc. Chem Res 37:471–478